Nanostructured high specific capacity C-$LiFePO_4$ cathode material for lithium-ion batteries

Khadije Bazzi, Kulwinder S. Dhindsa, Ambesh Dixit, Moodakere B. Sahana, and Chandran Sudakar
Department of Physics and Astronomy, Wayne State University, Detroit, Michigan 48201

Mariam Nazri
Applied Sciences Inc., Cedarville, Ohio 45314

Zhixian Zhou
Department of Physics and Astronomy, Wayne State University, Detroit, Michigan 48201

Prem Vaishnava
Department of Physics, Kettering University, Flint, Michigan 48504

Vaman M. Naik
Department of Natural Sciences, University of Michigan-Dearborn, Dearborn, Michigan 48128

Gholam A. Nazri and Ratna Naik[a)]
Department of Physics and Astronomy, Wayne State University, Detroit, Michigan 48201

(Received 1 May 2011; accepted 4 October 2011)

We report synthesis of nanosize $LiFePO_4$ and C-$LiFePO_4$ powders with a narrow particle size distribution (20–30 nm) by ethanol-based sol–gel method using lauric acid (LA) as a surfactant for high specific capacity lithium-ion battery cathode material. X-ray diffraction measurements demonstrated that the samples were single-phase materials without any impurity phases. The average crystallite size was found to decrease slightly from 29 nm to approximately 23 nm with carbon coating. The ratio of the Raman D-band (~1350 cm^{-1}) to G-band (~1590 cm^{-1}) intensities (I_D/I_G) and electronic conductivity of these materials show strong dependence on the amount of surfactant coverage. Remarkably, cell prepared with carbon-coated $LiFePO_4$ synthesized using 0.25 M solution of LA showed a very large specific capacity approaching the theoretical limit of 170 mAh/g, in stark contrast to the specific capacity of cell consisting of pure of $LiFePO_4$ (~75 mAh/g) measured at the same C/2 discharge rate.

I. INTRODUCTION

$LiFePO_4$ is a particularly advantageous cathode material for lithium-ion rechargeable batteries. Compared to conventional cathode materials, such as $LiCoO_2$ and $LiMn_2O_4$, it has improved capacity retention versus charge–discharge cycle numbers, particularly at elevated temperatures, and it is less toxic, more affordable, thermally stable, easily synthesized, and environmentally safe.[1–3] Particularly, $LiFePO_4$ is much safer at higher temperatures, owing to the thermal stability of PO_4^{3-} polyanion.[1] $LiFePO_4$ has an ordered olivine structure (S.G: *Pnma*) in which FeO_6 octrahedra share common corners in the *b–c* plane. The oxygen atoms in the crystal structure of $LiFePO_4$ are arranged in distorted, hexagonal close-packed arrangement, in which the lithium and the iron atoms occupy octahedral sites, whereas the phosphorous atoms occupy the tetrahedral sites. The strong P–O covalent bonds stabilize the antibonding Fe^{3+}/Fe^{2+} state through the Fe–O–X (X = P, S, As, Mo, or W) inductive effects to produce high operating potential. This results in a high lithium intercalation voltage of 3.4 V versus lithium metal. $LiFePO_4$ also has a high theoretical capacity of 170 mAh/g. However, its application as a cathode material has been largely hampered by its poor electrical conductivity (10^{-9} S/cm)[4] when compared to that of $LiCoO_2$ (10^{-3}S/cm)[5] and $LiMn_2O_4$ (10^{-5} S/cm).[6] Suboptimal rate capability and electrochemical performance of $LiFePO_4$ system are the consequences of its limited electrical conductivity.

Extensive research has been performed to enhance the electrical conductivity of $LiFePO_4$ including the use of dopants, metal dispersions, carbon coating, and the cosynthesis of the phosphate with carbon.[7–20] Yamada et al.[21] found that controlling the particle size by varying the annealing temperatures is important for the high performance of the $LiFePO_4$ cathode material. On the other hand, Chung and Chiang[22] found that by doping supervalent cations in $LiFePO_4$, the electronic conductivity can be enhanced by a factor of 10^6 and capacity can be increased to about 160 mAh/g at C/10 rate. Nonetheless, Nazar et al. attributed such an improvement in electronic conductivity to the formation of an iron phosphide phase during high

[a)]Address all correspondence to this author.
e-mail: rnaik@wayne.edu
DOI: 10.1557/jmr.2011.353

 © Materials Research Society 2011

https://doi.org/10.1557/jmr.2011.353 Published online by Cambridge University Press

annealing temperature (>600 °C).[23] Furthermore, Armand et al., by improving the kinetics of the electrochemical reaction and chemically coating $LiFePO_4$ with conducting carbon, achieved a capacity value almost equal to the theoretical capacity at 80 °C.[3,24,25] In addition, Delacourt et al.[26,27] synthesized carbon-free $LiFePO_4$ with a narrow particle size distribution by an aqueous precipitation method and delivered 140 mAh/g at C/10 rate. Recently, a low temperature polyol process[28] and sol–gel[29–33] technique have been successfully used in producing nanosized $LiFePO_4$ particles of 20- to 40-nm size with much more favorable electrochemical properties. It is well established that nanosize particles with conductive coating are required to obtain high-capacity due to the intrinsic poor electrical conductivity of polyanion cathodes.[4] Therefore, numerous synthetic techniques have been used to produce nanosize phosphate-based cathode materials, and different processes are utilized to improve electrical conductivity of this class of cathode materials. It is also crucial to make phase pure phosphate with olivine structure to achieve high electrochemical performances. Impurity phases such as iron oxides and other non-olivine phosphates are detrimental to cell cycle life.[18,34]

In this article, we report a novel, simple, inexpensive, durable, and easily reproducible surfactant-based sol–gel technique for the synthesis of pure $LiFePO_4$ and C-$LiFePO_4$ cathode materials. We used lauric acid (LA) as a precursor in various concentrations to achieve different carbon coverage for $LiFePO_4$ cathodes. We have demonstrated that electrochemical performance, particle morphology, and crystallite size of C-$LiFePO_4$ cathode material vary as a function of carbon coverage. We observe that excess carbon coverage lowers the capacity of C-$LiFePO_4$ material, which can be attributed to the reduction of the active component in the composite in conjunction with increasingly disordered carbon in the system. The optimum carbon coverage was obtained by incorporating 0.25 M LA precursor, which delivered a specific capacity very close to the theoretical limit of ~170 mAh/g at C/2 rate.

II. EXPERIMENTAL

$LiFePO_4$ and C-$LiFePO_4$ samples were prepared by sol–gel method with $CH_3CO_2Li.2H_2O$ (lithium acetate dehydrate, 99%; Alfa Aesar, Ward Hill, MA), $FeCl_2.4H_2O$ (ferrous chloride; Fisher Scientific, Pittsburgh, PA), and P_2O_5 (phosphorous pentoxide; Fisher Scientific) precursors. Each precursor was dissolved separately in ethanol (200 proof) to make 1 M solutions. The Fe and P solutions were first mixed in the desired stoichiometric ratio and stirred for 3 h followed by the addition of stoichiometric amount of the Li solution. After 3 h of stirring, 1 M solution of LA surfactant (Fisher Scientific) in ethanol was added to the main solution which was left for another 4 h to ensure the completion of the reaction to provide carbon shell structure on $LiFePO_4$ nanoparticle cores. To prevent the formation of Fe^{3+} impurities, the entire synthesis process was carried out under an inert atmosphere maintained by a continuous flow of nitrogen gas. The resulting sol was kept at 80 °C until it dried off completely. Three C-$LiFePO_4$ composite cathode materials with different amounts of carbon were prepared by setting the concentration of LA in the mixture to 0.25 M (sample B), 0.50 M (sample C), and 1.00 M (sample D), respectively. These dried sol nanopowders were annealed at 600 °C under the continuous flow of H_2/Ar (10%:90%) reducing gas for 5 h to obtain the single-phase materials avoiding the formation of Fe^{3+}-related complexes, except pure $LiFePO_4$ (sample A), which was annealed at 500 °C for 5 h under identical conditions.

The phase purity of the samples was verified by powder x-ray diffraction (XRD) using a Rigaku RU2000 rotating anode powder diffractometer (The Woodlands, TX). Raman spectra of all samples were measured using a Jobin–Yvon Horiba Triax 550 spectrometer (Edison, NJ), a liquid-nitrogen-cooled charge-coupled device detector, an Olympus model BX41 microscope (Center Valley, PA) with a 100× objective, and a 514.5 nm Modu-Laser (Stellar Pro-L) argon-ion laser (South Centerville, UT). The laser power at the sample was maintained at very low level (~1 mW) to avoid any heating effect. The Raman-scattered light from the sample was collected with the same microscope objective and focused on the entrance slit of the spectrometer with a 1200 line/mm diffraction grating. The data was recorded and analyzed by LabSpec software. The morphology and microstructure of the pure and three carbon-coated $LiFePO_4$ powders were investigated by using a JSM-6510LV-LGS scanning electron microscope (SEM; Peabody, MA) and a JEOL-2010 transmission electron microscope (TEM; Peabody, MA). A precision materials analyzer (Radiant Technologies, Albuquerque, NM) was used to measure the conductivity of all samples by attaching electrodes to the top and bottom of pressed pellets with conducting silver epoxy.

For electrochemical characterization, the cathodes were prepared by mixing 80 wt% of active material, 15 wt% of an expandable graphite as a conducting material, and 5 wt% of ethylene propylene diene monomer (M-class-terpolymer) as a binder. This composite was mixed with xylene (using micronizer mixer) to make homogenous slurry paint. The slurry paint was coated on graphitized aluminum (Al) foil, using a 15-μm-gap doctor blade draw-down technique over a vacuum bench to hold down the Al foil. The electrode was then dried inside a well-ventilated hood for at least 3 h to remove excess xylene, and subsequently transferred into a hot antechamber (110 °C) of a dry box and evacuated for at least 4 h. The dry sample was then transferred into a box filled with Argon with less than 1 ppm oxygen and moisture, where disk electrodes were cut and tested in coin cells against lithium counter electrode. We used the binary electrolyte consisting of ethylene carbonate (EC) and dimethyl carbonate solvents (DMC), (50:50) with 1 M

https://doi.org/10.1557/jmr.2011.353 Published online by Cambridge University Press

$LiPF_6$. The electrochemical properties of the cells were characterized using galvanostatic charge and discharge studies performed at a current of 0.1 mA with cut off voltages of 2.2–4.4 V at room temperature.

We measured the surface area of the pure $LiFePO_4$ and 0.25 M LA-coated $LiFePO_4$ samples using a Quantachrome Autosorb Automated Gas Sorption System (Boynton Beach, FL). We outgassed 0.5761 g of the pure $LiFePO_4$ sample at 150 °C for 39 h. The BET surface area of this sample was measured 3.33 m^2/g. Similarly, 0.6207 g of 0.25 M LA-coated $LiFePO_4$ sample was outgassed at 150 °C for 19 h, and a BET surface area of 54.13 m^2/g was obtained. The sample containing the 0.25 M LA provides the best electrochemical performance, close to theoretical capacity at C/2 rate. The surface areas for the 0.50 and 1.0 M LA-coated samples were found to be 68.14 and 74.12 m^2/g, respectively.

III. RESULTS AND DISCUSSION

The XRD patterns of one pure $LiFePO_4$ and three C-$LiFePO_4$ samples, shown in Fig. 1, are characteristic of the ideal orthorhombic olivine structure without any discernable impurity phases, where all the peaks can be indexed in the orthorhombic $LiFePO_4$ system with the Pnma space group (PDF No. 40-1499). We did not observe any major effects of carbon coating on the XRD of the cathode materials, except a minor change in the width of some of the peaks, suggesting that the coated carbon is largely amorphous. The crystallite size (D) was calculated from the Scherrer equation $\beta \cos(\theta) = k\lambda/D$, where β is the full-width-at-half-maximum of the XRD peak and k is a constant (~0.9).[35] The mean crystallite size D of the $LiFePO_4$ decreased from 29 nm to approximately 23 nm when LA was added during the synthesis. The addition of LA increased the residual carbon content. Specifically, in the three C-$LiFePO_4$ samples we get 3.7, 7.8, and 11.6 wt% of carbon corresponding to 0.25, 0.5, and 1 M LA, respectively. The room temperature electronic conductivities measured on the pellet synthesized with and without the surfactant are 5.0×10^{-8} and 6.4×10^{-4} S cm^{-1} for the pure $LiFePO_4$ and 0.25 M coated LA samples, respectively (Fig. 2). The four orders of magnitude higher conductivity of the 0.25 M treated sample in comparison with the pure $LiFePO_4$ sample suggests that a percolating network of carbon coating is formed to facilitate the charge transport. The conductivity value for pure $LiFePO_4$ is also somewhat higher than the literature value,[4] which could be partially due to the presence of a small amount of Fe_2P metallic magnetic impurity phase (having high electrical conductivity ~5.2×10^{-2} S cm^{-1} in pressed powder forms) in the cathode material.[23] Although the amount of Fe_2P impurities was so minute that the XRD measurements did not indicate the presence of the strongest (111) peak corresponding to the phosphides near 2θ angles in the range of 40.28–42.39°,[18] our Mossbauer spectroscopy measurement (A. Dixit et al., unpublished data) indeed revealed the presence of a phosphide peak in the form of a quadrupole doublet. The presence of Fe_2P phase has been suggested to increase the electronic conductivity,[23] with respect to other insulating iron oxide phases, which usually hamper electronic conductivity and thus electrochemical performance. Using the sensitivity of Fe^{57} Mossbauer spectroscopy, we identified four iron-containing phases in the pure and carbon-coated cathode materials (A. Dixit et al., unpublished data). These are Fe^{2+} in $LiFePO_4$, Fe_2P, γ-Fe_2O_3, and Fe phases. The amount of Fe^{2+} varied between 80 and 85% in the samples. There was no Fe_2P phase identified in the pure $LiFePO_4$ sample. The amount of Fe_2P remained practically constant at 9% in the three carbon-coated samples. The amount of iron oxide varied between 0 and 4%, and the metallic Fe phase varied between 9 and 4% for the 0.25, 0.50, and 1 M samples, respectively. Thus, for the majority of the impurity phases, Fe_2P and Fe, the d-electrons of iron will be delocalized extending the d-electron wave functions over

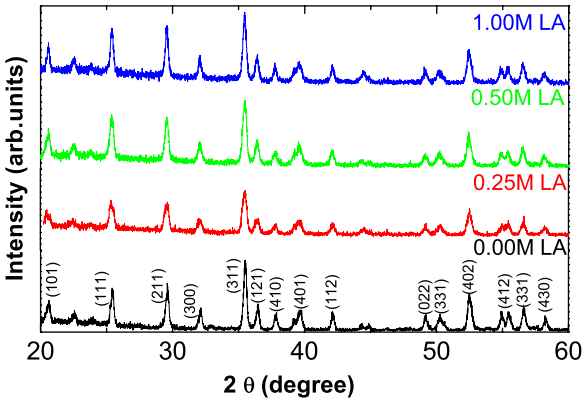


FIG. 1. Powder x-ray diffraction patterns of pure $LiFePO_4$ (samples A) and three different carbon-coated $LiFePO_4$ samples B (0.25M LA), C (0.50M LA), and D (1.0 M LA), respectively.

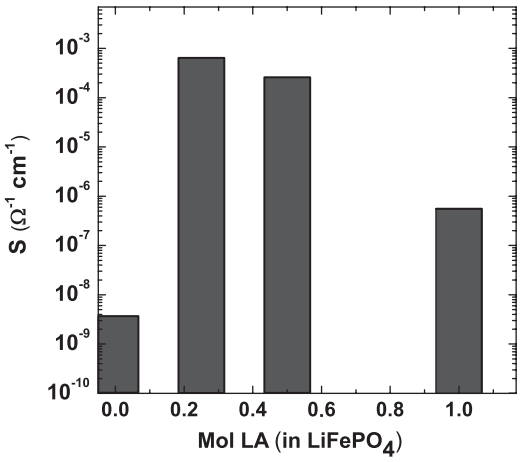


FIG. 2. Conductivity of pure $LiFePO_4$ (sample A) and three different C-$LiFePO_4$ samples B (0.25M LA), C (0.50M LA), and D (1.0M LA), respectively.

https://doi.org/10.1557/jmr.2011.353 Published online by Cambridge University Press

many iron sites, which would affect the conducting and electrochemical properties of the carbon-coated samples. It appears that the effects of Fe_2P impurity phase in influencing the conducting and electrochemical properties would be about the same but may be different when considering the Fe impurity phase. We speculate that the presence of residual metallic iron is due to a carbothermal reduction of iron oxide with reactive carbon that is formed by thermal decomposition of LA during heating process.

The morphology and the microstructure of the pure and carbon-coated $LiFePO_4$ samples analyzed by SEM measurements are shown in Figs. 3(a), 3(e), and 3(g), respectively. It is clear that the average size of the nanoparticles in the carbon-coated sample is smaller than that in pure $LiFePO_4$ suggesting that the addition of LA inhibits the particle size growth. The corresponding TEM images for pure and carbon-coated LiFePO4 samples [Figs. 3(b), 3(f), and 3(h)] show that the nanosized particles are highly spherical with smooth surfaces and are well dispersed for lower LA carbon-coated samples. Additionally, we also observed the onset of small nonuniformity in the size of particles for higher LA carbon-coated $LiFePO_4$ sample [Fig. 3(h)]. The representative electron diffraction pattern and high-resolution TEM micrograph, shown in Figs. 3(c) and 3(d) respectively, suggest that these $LiFePO_4$ nanoparticles are highly crystalline. We do not observe any discernible carbon coating on pure $LiFePO_4$ nanoparticles [Fig. 3(b)]. On the other hand, the carbon-coated $LiFePO_4$ nanoparticles are uniformly covered with an about 4-nm-thick layer of carbon, as shown in Fig. 3(f), which appears to be favorable for lithium-ion transport across the interface between $LiFePO_4$ and the electrolyte in addition to the enhanced electronic conductivity. The surface of the nanoparticles also contains nanorods of Fe_2P as indicated by the arrows in the Fig. 3(f). Such crystallites/nanorods have previously been reported in another study[36,37] and have been suggested to enhance conducting property of the cathode materials. The SEM/TEM micrographs for $LiFePO_4$ samples with higher carbon concentration [Fig. 3(h)] exhibit large clusters with nonuniform carbon coverage unlike the 0.25 M LA-carbonated $LiFePO_4$ sample. The structure of the carbon, particularly the sp^3/sp^2 disordered/graphitic (D/G) ratio, strongly influences the electronic conductivity of the cathodes. Samples containing smaller amounts of high-quality carbon (graphitic) can outperform those containing larger amounts of less-conducting carbon (disordered). It has been shown that the structure of the carbon in the composite cathode materials strongly depends on the nature of the carbon source (organic or polymeric precursor) and the processing conditions. The excess of carbon coverage has been known to change the diffusion length and reduce ionic conduction.[38]

Figure 4 shows the Raman spectra of pure $LiFePO_4$ sample (annealed at 500 °C) and three C-$LiFePO_4$ samples (annealed at 600 °C) in the 500–1700 cm^{-1} region. The observed low wavenumber Raman vibrational modes

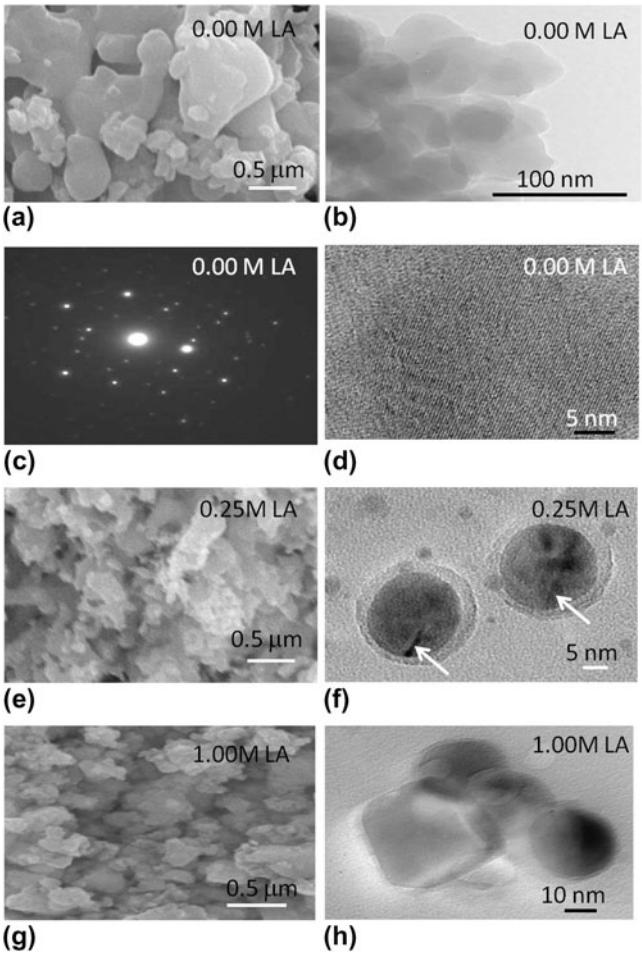


FIG. 3. (a), (e), and (g) are SEM images and (b), (f), and (h) are TEM images of pure $LiFePO_4$, 0.25 M LA and 1.00 M LA-carbon coated $LiFePO_4$ samples, respectively. (c) Selected area electron diffraction pattern of $LiFePO_4$ crystallites from pure $LiFePO_4$ sample, and (d) high-resolution TEM image for pure $LiFePO_4$ crystallite.

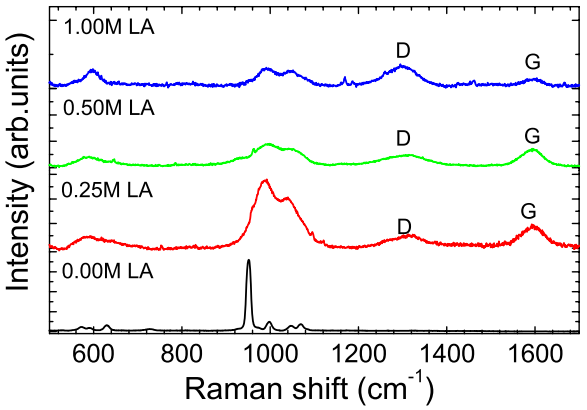


FIG. 4. The characteristic Raman vibrational spectra for samples A (pure $LiFePO_4$), B (0.25 M LA), C (0.50 M LA), and D (1 M LA) in the range 500–1700 cm^{-1}.

https://doi.org/10.1557/jmr.2011.353 Published online by Cambridge University Press

(below 500 cm^{-1}) are not shown here. However, they are in good agreement with the reported values.[38] The representative Raman spectrum for $LiFePO_4$ sample, shown in bottom panel of Fig. 4, consists of a strong Raman mode ~950 cm^{-1} [A_g(9)] along with 998 cm^{-1} [A_g(10)], 1047 cm^{-1} [A_g(11)], and 1069 cm^{-1} [B_{2g}(11)] modes[39] without any discernible signature for possible carbon-associated Raman modes. The A_g(9) mode shifts toward higher energy ~990 cm^{-1}, and its energy remains nearly independent of carbon concentration in $LiFePO_4$. More interestingly, there is a significant drop in the intensity of A_g(9) Raman mode after carbon functionalization and reduces continuously with increased carbon concentration in $LiFePO_4$. In addition to this A_g(9) mode, we also observed a broad peak centered at ~1040 cm^{-1}, indicating the smearing of A_g(10), A_g(11), and B_{2g}(11) Raman modes. The observed shift in the A_g(9), A_g(10), A_g(11), and B_{2g}(11) modes and strong reduction in their intensity after carbon coating suggests a strong carbon bonding with $LiFePO_4$ lattice. Additionally two intense broad peaks at ~1350 and ~1590 cm^{-1}, assigned to the D- and G-bands of residual carbon,[40] respectively, have been found to depend strongly on the carbon content in the samples. These two bands represent the fingerprints of the amorphous and graphitic carbon content present in the surface layers of these particles. Figure 4 illustrates the change of the shapes of the D- (sp^3-type carbon) and G-bands (sp^2-type carbon) for the three carbon-coated samples. To evaluate the effect of carbon coverage, we calculated the D-band to G-band intensity ratios, I_D/I_G, for the 0.25, 0.5, and 1 M C-$LiFePO_4$ samples, which are 0.750, 0.817 and 0.833, respectively. It appears that a thinner uniform carbon coat on the $LiFePO_4$ nanoparticles is responsible for an enhanced electrochemical characteristics. It is well known that the I_D/I_G Raman intensity ratio decreases as the carbon coating becomes less disordered (more graphitic), leading to the enhancement of the electronic conductivity and higher performance of the $LiFePO_4$ composite electrode. This is consistent with our finding that the $LiFePO_4$ sample with the addition of 0.25 M LA has the largest electrochemical capacity and the lowest I_D/I_G intensity ratio among all samples.

Figure 5(a) shows the galvanostatic charge–discharge profiles of the four $LiFePO_4$ cathode samples, A, B, C, and D, measured at C/2 between 2.2 and 4.4 V versus Li. The $LiFePO_4$ synthesized without surfactant (sample A) yielded only ~75 mAh/g at C/2 rate. The specific capacity improved when LA was introduced to the $LiFePO_4$ material. At C/2 rate, specific capacity was 100 mAh/g for the 1 M and 140 mAh/g for 0.5 M LA precursor solutions. The $LiFePO_4$ synthesized with 0.25 M surfactant exhibited significantly better electrochemical performance with a specific capacity of ~170 mAh/g, very close to the theoretical limit. This significant improvement in the electrochemical kinetics of the C-$LiFePO_4$ powders could be attributed to a number of

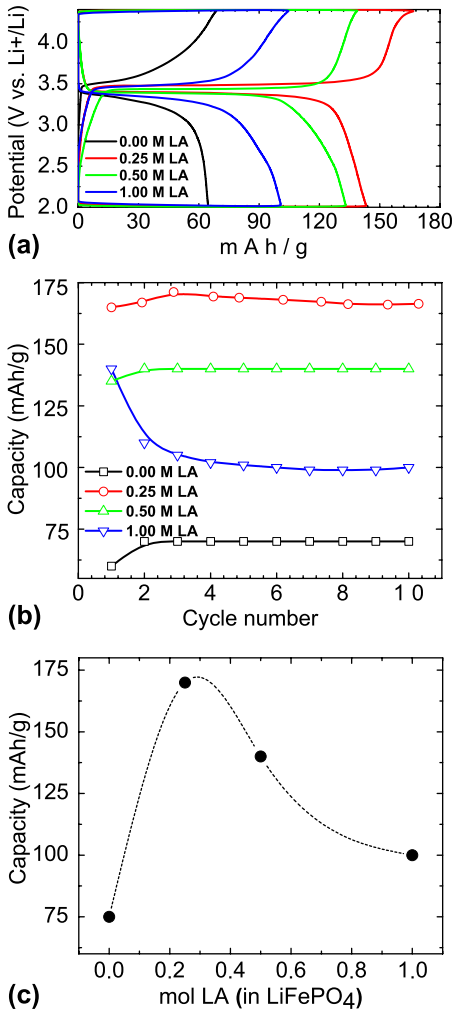


FIG. 5. (a). The voltage profile recorded during charge–discharge versus the specific capacity; (b) the discharge-specific capacity versus the cycle number for pure and different concentration of lauric acid (LA) surfactant carbon-coated $LiFePO_4$ samples; and (c) capacity versus molar fraction of LA used for the synthesis of these carbon-coated $LiFePO_4$ samples.

factors, such as improved surface area, reduced particle size, and the porous structure of the phosphates, as well as formation of a more conductive carbon coating. The increased value of the specific surface area along the *a*–*c* plane caused by a narrow distribution of nanosized particles would tend to offset the barriers to high rates governed by both the poor intrinsic electronic and ionic conductivities of the phosphates.[26,41,42] The electronic diffusion coefficient in the olivine $LiFePO_4$ cathode is known to be 8×10^{-18} m^2 s^{-1}, and the Li^+ diffusion coefficient in the $LiFePO_4$ and close to fully charged $FePO_4$ phases is found to be 1.8×10^{-18} and 2.2×10^{-20} m^2 s^{-1}, respectively.[43] By comparison, the Li^+ ion and electronic conductivities are in the same range of magnitude; it would be important to shorten both electronic and ionic paths within the particles[44,45] to achieve better conducting behavior of the material. In the case

https://doi.org/10.1557/jmr.2011.353 Published online by Cambridge University Press

of pure $LiFePO_4$, the particles have wide size distribution. Therefore, the smaller particles will be lithiated faster than the larger ones particularly during fast discharge/charge reaction, and the $LiFePO_4$ near the center of the larger particle will thus contribute very little to the redox reaction.

By adding surfactant to the pure cathode material, we inhibited particle size growth and created a porous structure for the 0.25 M sample to achieve unhindered transport of electrolyte into the particle's exterior.[15,17] In addition, we increased the surface area from 3.33 m^2/g for pure $LiFePO_4$ to 55.41 m^2/g for the 0.25 M LA-carbonated $LiFePO_4$ sample. This feature has a direct consequence to the electrochemical performance (specific capacity ~170 mAh/g) among the four samples investigated in this study. The porosity and the thickness of cathode play an important role in the electrochemical and conducting properties of the electrodes in Li-ion batteries. Small pore size has been shown to produce better electronic conductivity but not so good ionic conductivity. In a recent study[46] on a composite material $Li/LiPF_6$:(EC and DMC; 2:1 v/v)/$Li(Ni_{1/3}Mn_{1/3}Co_{1/3})O_2$/Al, it was noticed that the active electrode material [volume fraction percentage (vf%)] increases almost linearly with decreasing porosity (vf%). Therefore, there is a trade-off between the ionic conductivity of the electrolyte phase and electronic conductivity of the solid phase. The porosity also influences the utilization of the cathode materials. In one-dimensional simulation, it was found that at C/10 rate, the lower porosity shows better capacity.[46] However, as the C-rate increases, the higher porous electrode has higher capacity. The sample B with 0.25 M carbon additive has the best electronic conductivity and the C-rate among the four samples. But, adding more carbon to the sample not only reduces conductivity and C-rate but also penalizes the gravimetric properties irrespective of enhanced surface area for 0.75 and 1.00 M LA carbon-coated samples.

Figure 5(b) shows a plot of capacity versus cycle number for $Li/LiFePO_4$ cells containing different concentrations of LA surfactant additives. It shows clearly that the specific capacity of the C-$LiFePO_4$ with 1.00 M LA decreased faster during the early cycles, signifying high contact and matrix resistance related to the poor electronic conductivity of the carbon-rich phosphate.[40] However, the specific capacity of the 0.5 and 0.25 M LA-surfacted $LiFePO_4$ slightly increased with the early cycles and remains almost constant with the number of cycles for all the samples. The specific capacity of the sample with 0.25 M LA concentration was found to be the highest, approaching the theoretical value of ~170 mAh/g. The specific capacity decreased with further increasing LA concentration, as shown in Figs. 5(b) and 5(c). The constant value of the specific capacity with cycling numbers for all the four cathode materials validates the uniform and nanosized nature of the $LiFePO_4$ particles. The observed excellent cycling characteristics combined with improved kinetics of $LiFePO_4$ confirm the importance of optimizing the particle size and porosity of the $LiFePO_4$ electrode material synthesized using LA as the surfactant. Also, improvement in electronic conductivity through effective carbon coating by varying the amount of surfactant could further optimize the rate capability. As a continuation of the current study, the effect of various carboxylic acids, such as myristic and oleic acids, on the microstructure and electrochemical performance is being investigated presently and will be reported subsequently.

IV. CONCLUSION

Nanostructured $LiFePO_4$ and three C-$LiFePO_4$ powders were prepared by a sol–gel method using LA as the surfactant. The three C-$LiFePO_4$ synthesized with LA delivered specific capacity values of 100, 140, and 170 mAh/g for 1, 0.5, and 0.25 M surfactant concentration at a discharge rate of C/2, respectively, which is significantly better compared to the phosphate obtained without any surfactant (~75 mAh/g). These results show that the rate of performance for $LiFePO_4$ cathode can be enhanced by optimizing the particle size and porosity of $LiFePO_4$ particles through treatment with a suitable surfactant. The major advantage of the current sol–gel approach is the formation of a porous networked structure with uniform particle size by utilizing a carboxylic acid surfactant, which acts as a capping agent, preventing and minimizing the agglomeration of the phosphate particles.

ACKNOWLEDGMENTS

We thank Robert Cunningham from Kettering University for assisting with SEM work. We are also thankful to the Richard Barber Foundation for the financial support to perform this work.

REFERENCES

1. A.K. Padhi, K.S. Nanjundaswamy, and J.B. Goodenough: Phospho-olivines as positive-electrode materials for rechargeable lithium batteries. *J. Electrochem. Soc.* **144**, 1188 (1997).
2. N. Terada, T. Yanagi, S. Arai, M. Yoshikawa, K. Ohta, N. Nakajima, and N. Arai: Development of lithium batteries for energy storage and EV applications. *J. Power Sources* **100**, 80 (2001).
3. K.A. Striebel, A. Guerfi, J. Shim, M. Armand, M. Gauthier, and K. Zaghib: $LiFePO_4$/gel/natural graphite cells for the BATT program. *J. Power Sources* **119–121**, 951 (2003).
4. P.P. Prosini, D. Zane, and M. Pasquali: Improved electrochemical performance of a LiFePO4-based composite cathode. *Electrochim. Acta* **46**, 3517 (2001).
5. J. Molenda, A. Stoklosa, and T. Bak: Modification in the electronic structure of cobalt bronze LixCoO2 and the resulting electrochemical properties. *Solid State Ion.* **36**, 53 (1989).
6. Y. Shimakawas, T. Numata, and J. Tabuchi: Verwey-type transition and magnetic properties of the $LiMn_2O_4$ spinels. *J. Solid State Chem.* **131**, 138 (1997).
7. S.Y. Chung, J.T. Bloking, and Y-M. Chiang: Electronically conductive phosphor-olivines as lithium storage electrodes. *Nat. Mater.* **1**, 123 (2002).

https://doi.org/10.1557/jmr.2011.353 Published online by Cambridge University Press

8. J. Barker, M.Y. Saidi, and J.L. Swoyer: Lithium iron (II) phosphor-olivines prepared by a novel carbothermal reduction method. *Electrochem. Solid-State Lett.* **6**, A53 (2003).
9. M.M. Doeff, Y. Hu, F. McLarnon, and R. Kosteckl: Effect of surface carbon structure on the electrochemical performance of LiFePO$_4$. *Electrochem. Solid-State Lett.* **6**, A207 (2003).
10. H. Gabrisch, J.D. Wilcox, and M.M. Doeff: Carbon surface layers on a high-rate LiFePO$_4$. *Electrochem. Solid-State Lett.* **9**, A360 (2006).
11. F. Croce, A.D. Epifanio, J. Hassoun, A. Deptula, T. Olczac, and B. Scrosati: A novel concept for the synthesis of an improved LiFePO$_4$ lithium battery cathode. *Electrochem. Solid-State Lett.* **5**, A47 (2002).
12. G.X. Wang, L. Yang, Y. Chen, J.Z. Wang, S. Bewlay, and H.K. Liu: An investigation of polypyrrole-LiFePO4 composite cathode materials for lithium-ion batteries. *Electrochim. Acta* **50**, 4649 (2005).
13. G.X. Wang, S.L. Bewlay, K. Konstantinov, H.K. Liu, S.X. Dou, and J-H. Ahn: Physical and electrochemical properties of doped lithium iron phosphate electrodes. *Electrochim. Acta* **50**, 443 (2004); Yet-Ming Chiang, Anthony E. Pullen, Nonglak Meethong. US Patent Application 20070292747, December 20, 2007.
14. X-Z. Liao, Z-F. Ma, Y-S. He, X-M. Zhang, L. Wang, and Y. Jiang: Electrochemical behavior of LiFePO$_4$/C cathode material for rechargeable lithium batteries. *J. Electrochem. Soc.* **152**, A1969 (2005).
15. R. Dominko, J.M. Goupil, M. Bele, M. Gaberseek, M. Remskar, D. Hanzel, and J. Jamnik: Impact of LiFePO$_4$/C composites porosity on their electrochemical performance. *J. Electrochem. Soc.* **152**, A858 (2005).
16. G.X. Wang, L. Yang, S.L. Bewlay, Y. Chen, H.K. Liu, and J.H. Ahn: Electrochemical properties of carbon coated LiFePO$_4$ cathode materials. *J. Power Sources* **146**, 521 (2005); Michel Armand, John B. Goodenough, Akshaya Padhi, Kirakodu Nanjundaswamy, Christian Masquelier. US Patent Application 20050003274, January 6, 2005.
17. M. Takahashi, S. Tobishima, K. Takei, and Y. Sakurai: Characterization of LiFePO$_4$ as the cathode material for rechargeable lithium batteries. *J. Power Sources* **97–98**, 508 (2001).
18. G. Arnold, J. Garche, R. Hemmer, S. Strobele, C. Vogler, and M. Wohlfahrt-Mehrens: Fine-particle lithium iron phosphate LiFePO synthesized by a new low-cost aqueous precipitation technique. *J. Power Sources* **119–121**, 247 (2003).
19. A.D. Spong, G. Vitins, and J.R. Owen: A solution-precursor synthesis of carbon-coated LiFePO$_4$ for Li-ion cells. *J. Electrochem. Soc.* **152**, A2376 (2005).
20. Y. Hu, M.M. Doeff, R. Kostecki, and R. Finones: Electrochemical performance of sol-gel synthesized LiFePO$_4$ in lithium batteries. *J. Electrochem. Soc.* **151**, A1279 (2004).
21. A. Yamada, S-Y. Chung, and K. Hinokuma: Optimized LiFePO$_4$ for lithium battery cathodes. *J. Electrochem. Soc.* **148**, A224 (2001).
22. S.Y. Chung and Y.M. Chiang: Microscale measurements of the electrical conductivity of doped LiFePO$_4$. *Electrochem. Solid-State Lett.* **6**, A278 (2003).
23. P. Subramanya Herle, B. Ellis, N. Coombs, and L.F. Nazar: Nano-network electronic conduction in rion and nickel olivine phosphates. *Nat. Mater.* **3**, 147 (2004).
24. N. Ravet, S. Besner, M. Simoneau, A. Vall′ee, M. Armand, and J-F. Magnan: Hydro-Qu′ebec, Canadian Patent # CA2270771, 1999, 2, 270, 771.
25. N. Ravet, J.B. Goodenough, S. Besner, M. Simoneau, P. Hovington, and M. Armand: Improved iron based cathode materials. Abstract 127, The 196th Electrochemical Society and the Electrochemical Society of Japan Meeting Abstracts, Vol. 99–102, Honolulu, HI, October 17–22, 1999.
26. C. Delacourt, P. Poizot, S. Levasseur, and C. Masquelier: Size effects on carbon-free LiFePO4 powders—The key to superior energy density. *Electrochem. Solid-State Lett.* **9**, A352 (2006).
27. C. Delacourt, P. Poizot, M. Morcrette, J-M. Tarascon, and C. Masquelier: One-step low-temperature route for the preparation of electrochemically active LiMnPO$_4$ powders. *Chem. Mater.* **16**, 93 (2004).
28. D-H. Kim and J. Kim: Synthesis of LiFePO4 nanoparticles in polyol medium and their electrochemical properties. *Electrochem. Solid-State Lett.* **9**, A439 (2006).
29. R. Dominko, M. Bele, M. Gaberscek, M. Remskar, D. Hanzel, J.M. Goupil, S. Pejovnik, and J. Jamnik: Porous olivine composites synthesized by sol-gel technique. *J. Power Sources* **153**, 274 (2006).
30. J.S. Yang and J.J. Xu: Synthesis and characterization of carbon-coated lithium transitional metal phosphates LiMPO$_4$ (M = Fe, Mn, Co, Ni) prepared via a nonaqueous sol-gel route. *J. Electrochem. Soc.* **153**, A716 (2006).
31. M.A.E. Sanchez, G.E.S. Brito, M.C.A. Fantini, G.F. Goya, and J.R. Matos: Synthesis and characterization of LiFePO$_4$ prepared by sol-gel technique. *Solid State Ion.* **177**, 497 (2006).
32. Z.P. Guo, H. Liu, S. Bewlay, H.K. Liu, and S.X. Dou: A new synthetic method for preparing LiFePO4 with enhanced electrochemical performance. *J. New Mater. Electrochem. Syst.* **6**, 259 (2003).
33. D. Choi and P.N. Kumta: Surfactant based sol-gel approach to nanostructured LiFePO$_4$ for high rate Li-ion batteries. *J. Power Sources* **163**, 1064 (2007).
34. A.A. Salah, A. Mauger, C.M. Julien, and F. Gendron: Nano-sized impurity phases in relation to the mode of preparation of LiFePO$_4$. *Mater. Sci. Eng., B* **129**, 232 (2006).
35. Y. Xia, M. Yoshio, and H. Noguchi: Improved electrochemical performance of LiFePO4 by increasing its specific surface area. *Electrochim. Acta* **52**, 240 (2006).
36. Y. Rho, L.F. Nazar, L. Perry, and D. Ryan: Surface chemistry of LiFePO$_4$ studied by Mossbauer and X-ray photoelectron spectroscopy and its effect on electrochemical properties. *J. Electrochem. Soc.* **154**, A283 (2007).
37. C.W. Kim, J.S. Park, and K.S. Lee: Effect of Fe_2P on the electron conductivity and electrochemical performance of LiFePO$_4$ synthesized by mechanical alloying using Fe^{3+} raw material. *J. Power Sources* **163**, 144 (2006).
38. A. Peters, C. Kortes, D. Hesse, N. Zakharov, and J. Janek: Ionic conductivity and activation energy for oxygen ion transport in superlattices -The multilayer system CSZ (ZrO_2 + CaO)/Al_2O_3. *Solid State Ion.* **178**, 67 (2007).
39. S. Shi, H. Zhang, X. Ke, C. Ouyang, M. Lei, and L. Chen: First principles study of lattice dynamics of LiFePO$_4$. *Phys. Lett. A* **373**, 4096 (2009).
40. S.W. Song, R.P. Reade, R. Kostecki, and K.A. Striebel: Electrochemical studies of the LiFePO4 thin films prepared with pulsed laser deposition. *J. Electrochem. Soc.* **153**, A12 (2006).
41. G. Chen, X. Song, and T.J. Richardson: Electron microscopy study of the LiFePO$_4$ to FePO$_4$ phase transition. *Electrochem. Solid-State Lett.* **9**, A295 (2006).
42. V. Srinivasan and J. Newman: Discharge model for the lithium iron-phosphate electrode. *J. Electrochem. Soc.* **151**, A1517 (2004).
43. P.P. Prosini, M. Lisi, D. Zane, and M. Pasquali: Determination of the chemical diffusion coefficient of lithium in LiFePO$_4$. *Solid State Ion.* **148**, 45 (2002).
44. S. Franger, F. Lecras, C. Bourbon, and H. Rouault: LiFePO$_4$ synthesis routes for enhanced electrochemical performance. *Electrochem. Solid-State Lett.* **5**, A231 (2002).
45. C.W. Wang, A.M. Sastry, K.A. Striebel, and K. Zaghib: Extraction of layerwise conductivities in carbon-enhanced multilayered LiFePO$_4$ cathodes. *J. Electrochem. Soc.* **152**, A1001 (2005).
46. Y.H. Chen, C.W. Wang, X. Zhang, and A.M. Sastry: Porous cathode optimization for lithium cells: Ionic and electronic conductivity, capacity and selection of materials. *J. Power Sources* **195**, 2851 (2010).

https://doi.org/10.1557/jmr.2011.353 Published online by Cambridge University Press